IET Communications

Research Article

IET Journals
The Institution of Engineering and Technology

Signal detection technique for asynchronous filtered multi-tone modulation-based mesh systems

ISSN 1751-8628
Received on 30th March 2014
Accepted on 2nd November 2014
doi: 10.1049/iet-com.2014.0736
www.ietdl.org

Seung-Min Shin[1], Joo-Hyung Choi[1], Chang-Hwan Park[2], Won-Young Yang[1], Yong-Soo Cho[1] ✉

[1]*School of Electrical and Electronic Engineering, Chung-Ang University, Seoul, 156–756, Korea*
[2]*Advanced Communication Technology Lab, LG Electronics, Seoul, 137-724, Korea*
✉ *E-mail: yscho@cau.ac.kr*

Abstract: In this study, the authors propose a signal detection technique of successive interference cancellation to reduce the effect of inter-symbol interference (ISI), which is caused by the time difference of arrivals among distributed nodes in an asynchronous wireless mesh network based on filtered multi-tone modulation. The proposed signal detection technique uses partial matrices of a transmission gain matrix to mitigate the ISI effect from the adjacent symbols. Under the assumption of perfect symbol time offset and channel estimation at each node, it is shown by simulation that the proposed technique can improve the bit error rate performance with lower complexity compared with the conventional technique.

1 Introduction

Wireless mesh networks (WMNs) are known to have various advantages of inexpensive construction cost, easy network maintenance, scalability, robustness and service coverage extension [1, 2]. Owing to these advantages, the WMN is considered to be a promising wireless technology for numerous scenarios such as broadband home networking, enterprise networking, tactical information and communication networks, wireless networks for public safety and broadband metropolitan area networks [3].

WMNs based on orthogonal frequency division multiple access (OFDMA) have been actively researched because of their capability of broadband transmission and flexible resource allocation. A single-frequency mesh network has been implemented to show the feasibility of distributed network synchronisation on an experimental open-source real-time hardware/software platform, EURECOM Testbed OpenAirInterface, where the MIMO-OFDMA technique is employed in the physical layer [3]. A signal detection algorithm called two-dimensional ordered successive interference cancellation has also been proposed to minimise the effect of the time difference of arrivals (TDoA) at the receiver side in a WMN [4]. However, the OFDMA-based WMNs have the following disadvantages: (1) significant mutual interference among the signals from different nodes, especially because of the TDoAs exceeding the cyclic prefix (CP), (2) spectral efficiency degradation because of the dynamically adjusted CP length [5] and (3) difficulty of distributed synchronisation [6, 7].

Compared with OFDMA-based WMNs, WMNs based on filtered multi-tone modulation (FMT) are less affected by TDoAs and carrier frequency offsets (CFOs) among nodes, because of the filtering process on each subchannel [8, 9]. Owing to the property of a high level of spectral containment in FMT, an FMT-based WMN will have the following advantages: (1) small mutual interference among the signals from different nodes with different TDoAs and CFOs, (2) robustness to inter-channel interference and inter-symbol interference (ISI) in an asynchronous multi-node scenario [8] and (3) no need for distributed synchronisation. Owing to these advantages, FMT-based WMNs will be suitable for opportunistic communication or cognitive radio systems that dynamically allocate the available resources for each node depending on the channel conditions and network traffic.

In this paper, we consider a signal detection technique for asynchronous FMT-based WMNs with TDoAs among distributed nodes. We propose a signal detection technique of successive interference cancellation (SIC) using partial matrices of a transmission gain matrix under the assumption of perfect symbol time offset (STO) and channel estimation at each node [10, 11]. By exploiting the fact that most of the ISI power is concentrated in the previous and next symbols, the proposed technique detects the signals successively with partial transmission gain matrices, reducing the effect of ISI caused by multipath fading channels and TDoAs among distributed nodes. The proposed technique can detect the multi-node signals simultaneously with reduced computational complexity. The performance of the proposed technique is evaluated by simulation with parameters from the 'TETRA' Enhanced Data Service, a commercial FMT transmission system.

This paper is organised as follows. In Section 2, the basic model of an FMT system is used to investigate how the TDoA affects the received signal in an FMT-based WMN system. Section 3 analyses the ISI effect depending on the value of the TDoA, and proposes a forward successive detection (FSD), backward successive detection (BSD), and bidirectional successive detection (BiSD) techniques for mitigating the ISI effect. Section 4 compares the bit error rate (BER) performance of conventional and proposed signal detection techniques through simulations, and compares their computational complexities. Conclusions are made in Section 5.

2 System model

In Fig. 1, we consider an FMT-based WMN system where a frame consists of N FMT symbols, each of which is composed of M subcarriers that are allocated among U nodes in an orthogonal manner in the frequency domain. Thus, M/U subcarriers will be allocated in a block type to each node. $A_{i|n}^{(u)}$ denotes the QAM symbol transmitted on the $i(\in I_u)$th subcarrier of the nth FMT symbol from node u every T seconds. I_u and T denote the set of subcarrier indices allocated to node u and the FMT symbol duration, respectively. In Fig. 1, each symbol $A_{i|n}^{(u)}$ (generated by node u for $i \in I_u$) is K-fold upsampled, passes through a Nyquist filter (with impulse response $h(mTc)$), and is then frequency-shifted by $2\pi f_i$. The transmitted baseband FMT signal

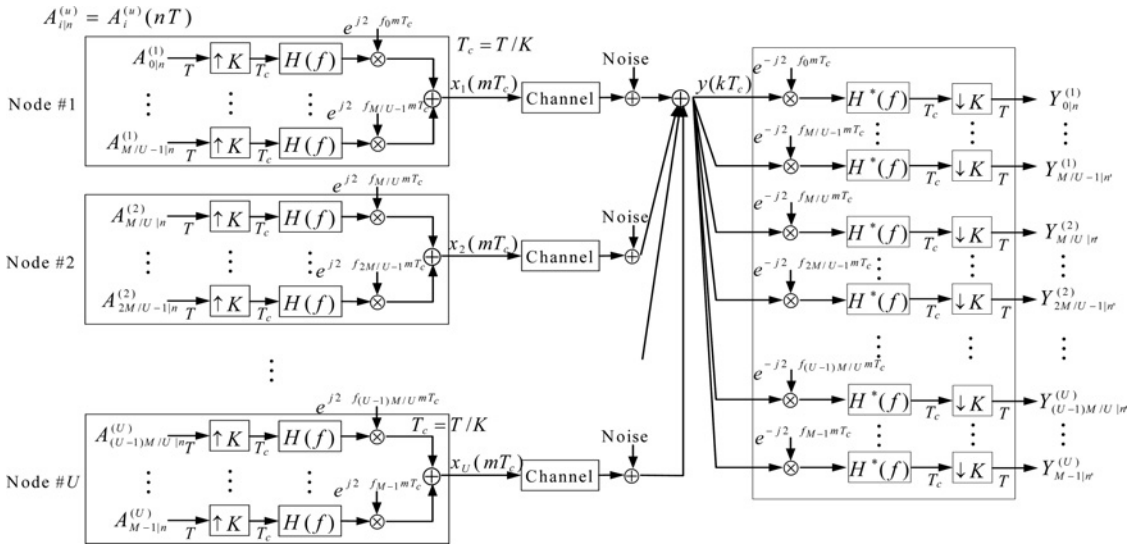

Fig. 1 *Block diagram of a multi-node FMT transmission system*

can be written as

$$x^{(u)}(mT_c) = \sum_{i=0}^{M-1} \sum_{n=-\infty}^{\infty} A_{i|n}^{(u)} h(mT_c - nT) \mathrm{e}^{\mathrm{j}2\pi im/M} \tag{1}$$

where $T_c(=T/K)$ denotes the transmission sampling interval. Also, the symbol $A_{i|n}^{(u)}$ on the subcarrier indices not allocated to node u is set to zero as

$$A_{i|n}^{(u)} = 0 \quad \text{for } i \notin I_u \tag{2}$$

The FMT signal in (1) is transmitted through a digital-to-analog converter and passes through a channel. The signal arriving at a receiver and passing through an analog-to-digital converter can be written as

$$r(mT_c) = \sum_{u=1}^{U} \sum_{l=0}^{L-1} x^{(u)}\big((m - l - \delta^{(u)})T_c\big) g_l^{(u)}(mT_c) + w(mT_c) \tag{3}$$

where L, $\delta^{(u)}$, $g_l^{(u)}(mT_c)$ and $w(mT_c)$ denote the number of multi-path components, the STO of node u, the channel impulse response of the lth path for node u and zero-mean additive white Gaussian noise (AWGN) with a variance $E\{|w(mT_c)|^2\} = \sigma^2$. As shown in Fig. 1, the received signal is frequency-shifted by $-2\pi f_i$ and passes through the matched filter (with impulse response $h^*(mT_c)$), and then is K-fold downsampled to yield the estimated symbols as

$$Y_{i|n}^{(u)} = \sum_{l=0}^{L-1} g_l^{(u)} \sum_{m=-\infty}^{\infty} x^{(u)}\big((m - l - \delta^{(u)})T_c\big) \mathrm{e}^{-\mathrm{j}2\pi im/M} h^*\big((m - Kn)T_c\big) + w(nT) \tag{4}$$

The estimated symbol can be written as [12] (see (5))

where $R_h(n)$ is the autocorrelation sequence of the transmit filter impulse response $h(n)$ defined as

$$R_h(n) = \sum_{m=-\infty}^{\infty} h\big((m - n)T_c\big) h^*(mT_c) \tag{6}$$

The transmission gain coefficient is defined as the Fourier transform of the weighted autocorrelation as follows

$$G_{i|n}^{(u)} = \sum_{l=0}^{L-1} g_l^{(u)} \mathrm{e}^{-\mathrm{j}2\pi i(l+\delta^{(u)})/M} R_h\big(l + \delta^{(u)} + nK\big) \tag{7}$$

(5) can be simplified as

$$Y_{i|n'}^{(u)} = G_{i|0}^{(u)} A_{i|n'}^{(u)} + \overbrace{\sum_{\substack{n=-\infty \\ n \neq n'}}^{\infty} G_{i|n-n'}^{(u)} A_{i|n'}^{(u)}}^{\text{ISI}} + w(n'T) \tag{8}$$

where the first, second and third terms denote the effect because of the effective channel, the ISI because of other symbols, and the noise, respectively. The second term will be zero in an AWGN environment, but in a multipath fading channel environment, it is contributed as an ISI whose magnitude and phase vary with the channel gain $g_l^{(u)}$ and propagation delay $\delta^{(u)}$ of the node u. Collecting (8) for N FMT symbols (constituting a frame) in a vector-matrix form yields

$$\boldsymbol{y}_i^{(u)} = \boldsymbol{W}_i^{(u)} \boldsymbol{a}_i^{(u)} + \boldsymbol{w} \tag{9}$$

where (see (10) at the bottom of the next page)

The coefficient matrix $\boldsymbol{W}_i^{(u)}$ in (10) is the transmission gain matrix for a frame. The diagonal and off-diagonal elements of $\boldsymbol{W}_i^{(u)}$ account for the effect of the channel and the ISI on the estimated symbols, respectively.

Before discussing the signal detection technique, the ISI effect because of TDoA is examined. Here, the raised cosine filter, currently used in the commercialised TETRA system, is used as

$$Y_{i|n'}^{(u)} = A_{i|n'}^{(u)} \sum_{l=0}^{L-1} g_l^{(u)} \mathrm{e}^{-\mathrm{j}2\pi i(l+\delta^{(u)})/M} R_h(l) + \overbrace{\sum_{\substack{n=-\infty \\ n \neq n'}}^{\infty} A_{i|n'}^{(u)} \sum_{l=0}^{L-1} g_l^{(u)} \mathrm{e}^{-\mathrm{j}2\pi i(l+\delta^{(u)})/M} R_h\big(l + \delta^{(u)} + (n - n')K\big)}^{\text{ISI}} + w(n'T) \tag{5}$$

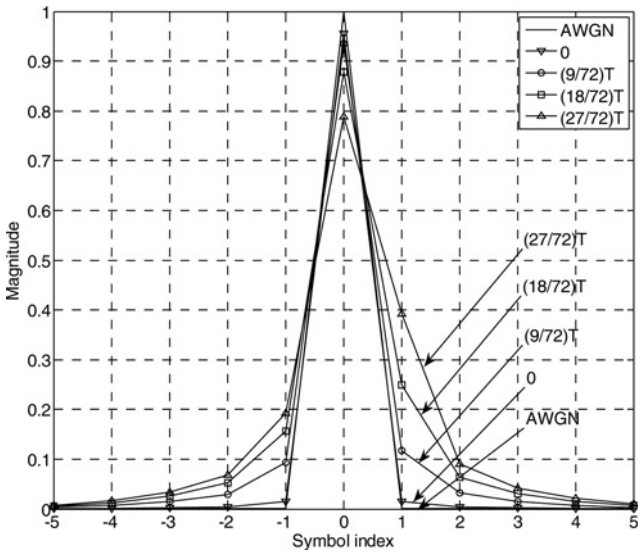

Fig. 2 *Effect of ISI depending on the propagation delay in the TETRA system*

the transmit and receive filter. Under the assumption of no channel and noise, the received FMT symbol has an envelope of the raised cosine filter with a magnitude inversely proportional to the sample index to the third power. Fig. 2 shows how the power of an FMT symbol arriving at the receiver is distributed over the previous and successive FMT symbol durations in an environment of AWGN/HT (Hilly Terrain) 200 channel. Most of the ISI power can be attributed to the neighbouring FMT symbols, especially to the one prior to the current FMT symbol if the propagation delay is not too large. As the propagation delay becomes large, the magnitude and range of the ISI power relative to the data power increase, as shown in Fig. 2.

3 Signal detection techniques for an asynchronous FMT-based mesh system

As a signal detection technique for an asynchronous FMT-based mesh system, we can consider the 'conventional signal detection (CSD)', which performs only one FFT operation with the FFT starting point at the arrival time of the signal from an arbitrary node and then estimates the transmitted symbol as

$$\tilde{\boldsymbol{a}}_i^{(u)} = \left[\boldsymbol{W}_i^{(u)}\right]^{-1} \boldsymbol{y}_i^{(u)} \tag{11}$$

Although this technique needs to compute the inverse of an $N \times N$ matrix (N: the number of FMT symbols per frame), it is expected to yield a poor performance because the FFT starting point is not synchronised with the other U-1 nodes.

Also, we can consider 'FFT for every node_signal detection (FENSD)', which performs the FFT operation to detect the signal from each node. In this technique, the required number of FFT operations is equal to U (the number of nodes). This technique can reduce the ISI term because of TDoA to a certain degree, but its computational complexity increases as the number of nodes increases. In this paper, it is assumed that the STOs of the received signals from neighbouring nodes are estimated in advance with the training sequences transmitted from neighbouring nodes. For instance, the STOs can be estimated by the technique in [13]. In this section, we propose a FSD, BSD, BiSD techniques for mitigating the ISI effect because of TDoA.

3.1 Forward successive detection

FSD takes the FFTs of the FMT symbols belonging to a frame arriving first among the ones from all the nodes and then, based on the partial transmission gain matrix (a fixed-size principal minor matrix of $\boldsymbol{W}_i^{(u)}$), applies the zero-forcing (ZF)-SIC scheme in the forward direction to reduce the effect of ISI and error propagation. The procedure can be described as follows (see Fig. 3*a*)

Step 1: Take the FFTs of N FMT symbols belonging to a frame arriving first among the ones from all nodes and construct $\boldsymbol{y}_i^{(u)}$ for $i = 1{:}M$ and for $u = 1{:}U$.

Step 2: Initialisation

1. Set the size q of the partial transmission gain matrix
2. Set $\hat{a}_i^{(u)}(k) = 0 \text{for} k \le 0$.

Step 3: Let $k = 1$.

Step 4:

$$\alpha = \boldsymbol{W}_i^{(u)}(2,1)\hat{A}_{i|k-1}^{(u)} + \boldsymbol{W}_i^{(u)}(3,1)\hat{A}_{ik-2}^{(u)} + \boldsymbol{W}_i^{(u)}(4,1)\hat{A}_{i|k-3}^{(u)} \tag{12a}$$

(ISI effect of three previously-detected FMT symbols)

Step 5: (see (12b))

Step 6:

$$\hat{\boldsymbol{a}}_i^{(u)}(k{:}k+q-1) = Q\left(\tilde{\boldsymbol{a}}_i^{(u)}(k{:}k+q-1)\right) \tag{12c}$$

Step 7: If $k = N - q + 1$, stop. Otherwise, let $k \leftarrow k + 1$ and go to Step 4.

where $Q(\cdot)$ denotes the slicing function. The size q of the partial transmission gain matrix can be made small or large as the value of TDoA becomes small or large. Note that the values of $\boldsymbol{W}_i^{(u)}(k{:}k+q-1,\ k{:}k+q-1)$ and $\{\boldsymbol{W}_i^{(u)}(2,1),\ \boldsymbol{W}_i^{(u)}(3,1),\ \boldsymbol{W}_i^{(u)}(4,1)\}$ do not vary with the FMT symbol index k if the channel is constant over one frame

$$\boldsymbol{W}_i^{(u)}(k{:}k+q-1,\ k{:}k+q-1) = \begin{bmatrix} G_{i|0}^{(u)} & \cdots & G_{i|q-1}^{(u)} \\ \vdots & \ddots & \vdots \\ G_{i|1-q}^{(u)} & \cdots & G_{i|0}^{(u)} \end{bmatrix} \tag{13}$$

$$\boldsymbol{y}_i^{(u)} = \begin{bmatrix} Y_{i|1}^{(u)} \\ Y_{i|2}^{(u)} \\ \vdots \\ Y_{i|N}^{(u)} \end{bmatrix},\ \boldsymbol{W}_i^{(u)} = \begin{bmatrix} G_{i|0}^{(u)} & G_{i|1}^{(u)} & \cdots & G_{iN-1}^{(u)} \\ G_{i|-1}^{(u)} & G_{i|0}^{(u)} & \ddots & \vdots \\ \vdots & \ddots & \ddots & G_{i|1}^{(u)} \\ G_{i|1-N}^{(u)} & \cdots & G_{i|-1}^{(u)} & G_{i|0}^{(u)} \end{bmatrix},\ \boldsymbol{a}_i^{(u)} = \begin{bmatrix} A_{i|1}^{(u)} \\ A_{i|2}^{(u)} \\ \vdots \\ A_{i|N}^{(u)} \end{bmatrix} \tag{10}$$

$$\tilde{\boldsymbol{a}}_i^{(u)}(k{:}k+q-1) = \left[\boldsymbol{W}_i^{(u)}(k{:}k+q-1,\ k{:}k+q-1)\right]^{-1}\left(\boldsymbol{y}_i^{(u)}(k{:}k+q-1) - \alpha\right) \tag{12b}$$

IET Commun., 2015, Vol. 9, Iss. 5, pp. 658–664

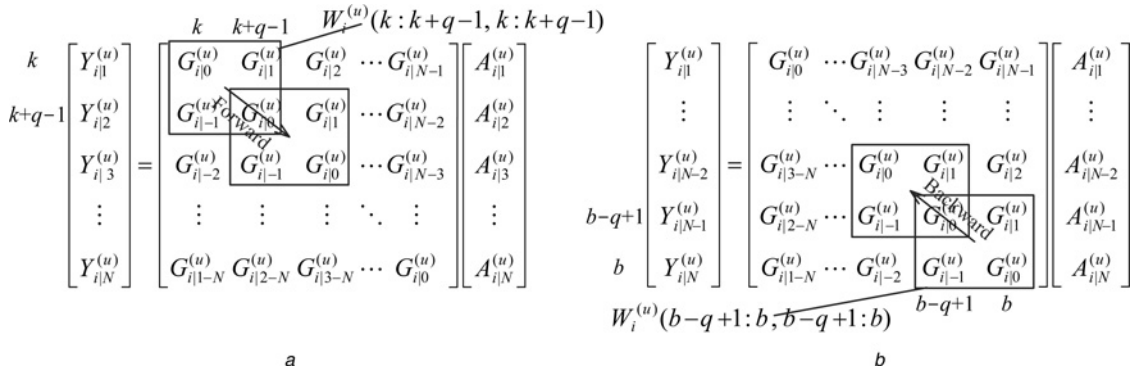

Fig. 3 *Partial transmission gain matrices used in FSD/BSD techniques*
a FSD
b BSD

$$\boldsymbol{W}_i^{(u)}(2,1) = G_{i|-1}^{(u)},\ \boldsymbol{W}_i^{(u)}(3,1) = G_{i|-2}^{(u)},\ \text{and}\ \boldsymbol{W}_i^{(u)}(4,1) = G_{i|-3}^{(u)} \tag{14}$$

3.2 Backward successive detection

BSD takes the FFTs of the FMT symbols belonging to a frame arriving last among the ones from all nodes, and then, based on the partial transmission gain matrix, applies the ZF-SIC technique in the backward direction to reduce the effect of ISI and error propagation. The procedure can be described as follows (see Fig. 3*b*):

Step 1: Take the FFTs of N FMT symbols belonging to a frame arriving last among the ones from all nodes and construct $\boldsymbol{y}_i^{(u)}$ for $i = 1{:}M$ and for $u = 1{:}U$.

Step 2:

1. Set the size q of the partial transmission gain matrix.
2. Set $\hat{a}_i^{(u)}(k) = 0$ for $k > N$.

Step 3: Let $b = N$.

Step 4:

$$\beta = \boldsymbol{W}_i^{(u)}(N-1, N)\hat{\boldsymbol{A}}_{i|b+2}^{(u)} + \boldsymbol{W}_i^{(u)}(N-2, N)\hat{\boldsymbol{A}}_{i|b+2}^{(u)} + \boldsymbol{W}_i^{(u)}(N-3, N)\hat{\boldsymbol{A}}_{i|b+3}^{(u)} \tag{15a}$$

(ISI effect of three previously-detected FMT symbols)

Step 5: (see (15b))

Step 6:

$$\hat{\boldsymbol{a}}_i^{(u)}(b-q+1:b) = Q\left(\bar{\boldsymbol{a}}_i^{(u)}(b-1+1:b)\right) \tag{15c}$$

Step 7: If $b = q$, stop. Otherwise, let $b \leftarrow b-1$ and go to Step 4.

In a similar way to FSD, the size q of the partial transmission gain matrix can be made small or large as the TDoA becomes small or large. Also, the values of $\boldsymbol{W}_i^{(u)}(b-q+1:b,\ b-q+1:b)$ and $\{\boldsymbol{W}_i^{(u)}(N-1, N),\ \boldsymbol{W}_i^{(u)}(N-2, N),\ \boldsymbol{W}_i^{(u)}(N-3, N)\}$ do not vary with the FMT symbol index k if the channel is constant over one frame

$$\boldsymbol{W}_i^{(u)}(b-q+1:b,\ b-q+1:b) = \begin{bmatrix} G_{i|0}^{(u)} & \cdots & G_{i|\,q-1}^{(u)} \\ \vdots & \ddots & \vdots \\ G_{i|\,1-q}^{(u)} & \cdots & G_{i|0}^{(u)} \end{bmatrix} \tag{16}$$

$$\boldsymbol{W}_i^{(u)}(N-1, N) = G_{i|\,1}^{(u)},\ \boldsymbol{W}_i^{(u)}(N-2, N) = G_{i|\,2}^{(u)},\ \text{and}\ \boldsymbol{W}_i^{(u)}(N-3, N) = G_{i|\,3}^{(u)} \tag{17}$$

3.3 Bidirectional successive detection

BiSD takes the FFTs of the FMT symbols belonging to the frame arriving first/last among the ones from all nodes, and then, applies the FSD/BSD algorithms for the subcarrier components belonging to the nodes. Fig. 4 shows an example of the received signals from four nodes with different STOs ($\delta^{(u)}$). The signals from nodes {1, 2} and {3, 4} are regarded as having arrived relatively earlier/later because their STOs are smaller/larger than the mid-value Δ of the smallest and largest STOs

$$\Delta = \frac{\Delta_{\mathrm{F}} + \Delta_{\mathrm{B}}}{2} \tag{18}$$

where Δ_{F} and Δ_{B} are the smallest and largest STOs, respectively

$$\Delta_{\mathrm{F}} = \min\{\delta^{(u)},\ u = 1, \ldots, U\} \tag{19a}$$

$$\Delta_{\mathrm{B}} = \max\{\delta^{(u)},\ u = 1, \ldots, U\} \tag{19b}$$

The BiSD technique applies the FSD/BSD algorithms to reconstruct the transmitted symbols for the subcarrier components belonging to the nodes from which the signal arrives with STO smaller/larger than Δ, respectively.

Compared with the case of FSD or BSD, the BiSD technique requires twice as many computations for FFT operation. For increased computations, its performance becomes better as the STO difference $\Delta_{\mathrm{B}} - \Delta_{\mathrm{F}}$ increases. However, the performance improvement may not be significant considering the increased computational complexity when the STO difference is not large. Therefore in the proposed approach, the BiSD technique is applied when the STO difference is larger than δth, a threshold value to be determined based on empirical or experimental data. Either the FSD or the BSD technique is applied when the STO difference is smaller than the threshold value. This allows the proposed

$$\bar{\boldsymbol{a}}_i^{(u)}(b-q+1:b) = \left[\boldsymbol{W}_i^{(u)}(b-q+1:b,\ b-q+1:b)\right]^{-1}\left(\boldsymbol{y}_i^{(u)}(b-q+1:b) - \beta\right) \tag{15b}$$

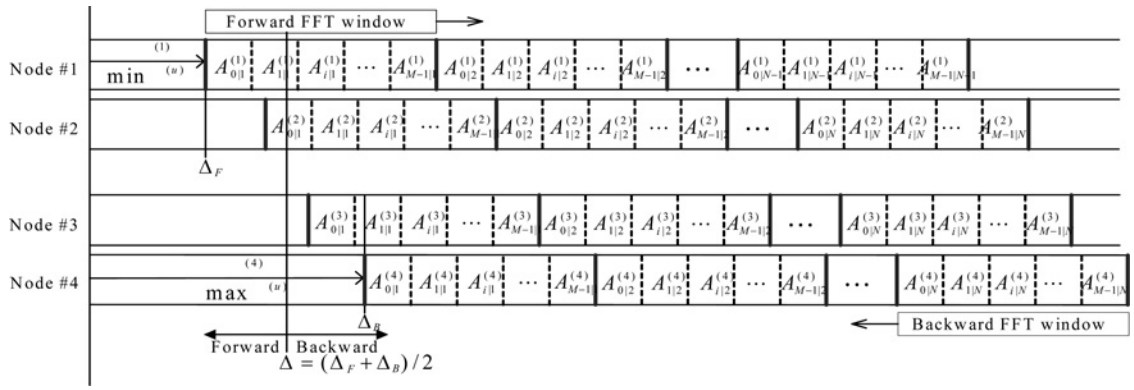

Fig. 4 *Example of received signals with different STOs*

technique to maintain a good balance between the performance and computational load.

Fig. 5 shows the procedure for choosing a signal detection technique in the proposed approach. First, either the FSD/BSD technique or BiSD technique is chosen depending on the STO difference. The FSD/BSD technique is applied when $\Delta_B - \Delta_F \leq \delta$th. Otherwise, the BiSD technique is applied. Next, If $\Delta_B - \Delta_F \leq \delta$th, then the FSD/BSD technique is chosen. Either the FSD or BSD technique is selected depending on the values of ξ_F and ξ_B, which are defined as

$$\xi_F = \sum_{i=0}^{M-1} \left| \sum_{\substack{n=-\infty \\ n \neq n'}}^{\infty} G_{i|n-n'}^{(u)|F} A_{i|n'}^{(u)} \right|^2 \tag{20}$$

$$\xi_B = \sum_{i=0}^{M-1} \left| \sum_{\substack{n=-\infty \\ n \neq n'}}^{\infty} G_{i|n-n'}^{(u)|B} A_{i|n'}^{(u)} \right|^2 \tag{21}$$

where $G_{i|n}^{(u)|F}$ and $G_{i|n}^{(u)|B}$ are obtained using (7) and (8) as follows

$$G_{i|n}^{(u)|F} = \sum_{l=0}^{L-1} g_l^{(u)} e^{-j2\pi i(l+\Delta_F)/M} R_h(l + \Delta_F + nK) \tag{22}$$

$$G_{i|n}^{(u)|B} = \sum_{l=0}^{L-1} g_l^{(u)} e^{-j2\pi i(l+\Delta_B)/M} R_h(l + \Delta_B + nK) \tag{23}$$

Here, $G_{i|n}^{(u)|F}$ and $G_{i|n}^{(u)|B}$ denote the transmission gain coefficients when the starting point is set with respect to the smallest STO and the largest STO in (7), respectively. Also, ξ_F denotes the ISI power obtained with the time delay Δ_F arriving first among the signals from all neighbouring nodes. ξ_B denotes the ISI power obtained with the time delay Δ_B arriving last among the signals. If $\xi_F \leq \xi_B$, the FSD technique is chosen. Otherwise, the BSD technique is chosen. Once a signal detection technique is chosen, either the FSD or BSD technique is applied to all nodes unlike the BiSD technique. Note that, in the BiSD technique, either the 'FSD' or 'BSD' technique is applied to each node depending on the estimated value of time delay. If it is not possible to find the threshold value δth, we can apply the BiSD technique because it always provides good performance with a slightly higher complexity.

4 Simulation

In this section, the performances of signal detection techniques are evaluated with the parameters and channel models used in the commercialised TETRA system. The modulation format is 4 or 64-QAM, the number of subcarriers M is 64, and the transmit and receive filters are the square root raised cosine filters with an upsampling factor $K = 72$ and a roll-off factor of 0.125. The subcarriers are evenly allocated to $U = 4$ users in a block type, the number N of FMT symbols per frame is 10, and the STOs of FMT signals from four nodes #1, #2, #3 and #4 are 0, (9/72)T, (18/72)T and (27/72)T, respectively. The threshold value δth is set to $T/4$ based on the experimental data from the commercialised TETRA system. The multipath fading channel used for simulation is HT200.

Fig. 6 shows BER performances of FSD, BSD and BiSD, all with $q = 2$, when 64-QAM and HT200 channel are used. The analytical curve for a Rayleigh channel is included for comparison. This figure shows that the BER performance of FSD/BSD for the node #1/#4 signals (FSD Node #1/BSD Node #4) that arrive first/last, respectively, are satisfactory, and close to the analytical curve. The BER performances of FSD/BSD for the node #4/#1 signals (FSD Node #4/BSD Node #1) are poor, yielding error floors. It also shows that the average BER performance of BiSD (BiSD Avg.) for all nodes is about 12 dB better than those of FSD (FSD Avg.) and BSD (BSD Avg.) at the BER of 10^{-2}.

The unbalanced shape of the ISI curve in Fig. 2 is attributed to the filter mismatch caused by the HT200 channel and propagation delay. It can be seen from Fig. 2 that the postcursor part increases faster than the precursor part as the propagation delay increases. It implies that the ISI effect because of the previous symbols is larger than that because of the successive symbols. It is for this reason that the BER performance of FSD technique is about 2 dB better than that of BSD technique as seen from Fig. 6. It can be also seen from Fig. 2 that the ISI because of the next symbol is 0.25 when the propagation delay is (18/72)T. The ISIs because of the next two symbols are 0.07 and 0.04, which are not ignorable. Therefore the size of the partial matrix must be increased to compensate for the ISI effect if the FSD/BSD technique is used. However, if BiSD technique is used, the ISI effect can be effectively reduced with a small size of the partial matrix.

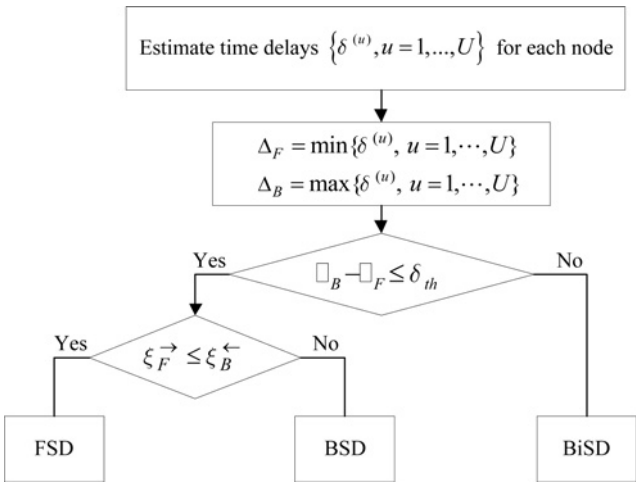

Fig. 5 *Procedure for choosing a signal detection technique*

IET Commun., 2015, Vol. 9, Iss. 5, pp. 658–664

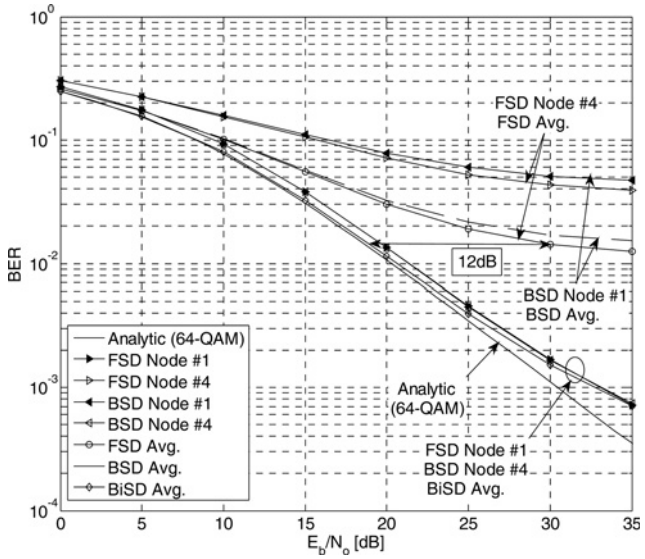

Fig. 6 *BER performance of FSD, BSD and BiSD techniques (2 × 2)*

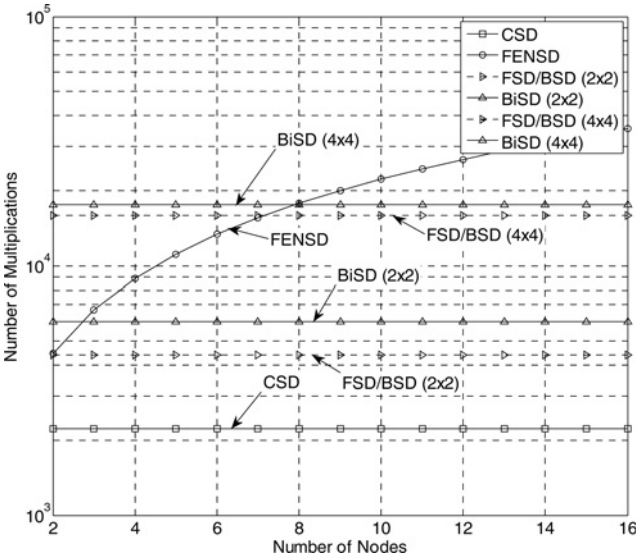

Fig. 8 *Number of multiplications against the number of nodes*

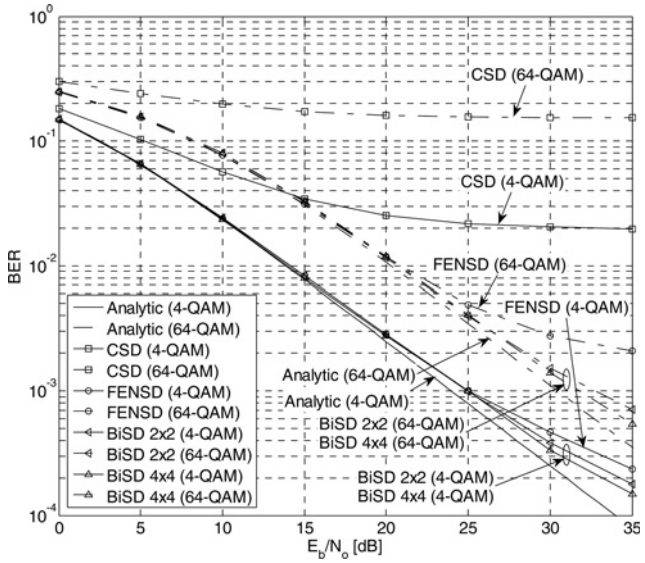

Fig. 7 *BER performance of conventional, FENSD and BiSD techniques*

Fig. 7 shows the BER performance of the conventional, FENSD and BiSD when an HT200 channel is used. The analytical curves for a Rayleigh fading channel are included for comparison using 4-QAM and 64-QAM. This figure shows that the conventional technique (CSD) yields error floors at $10^{-2}/10^{-1}$ for the cases of 4-QAM and 64-QAM, respectively. The performance of the FENSD technique for the case of 4-QAM/64-QAM signals is worse than that of BiSD, because of the ISI effect of the multipath channel. The BiSD technique performs best among the signal detection techniques discussed in this paper. The performance of the BiSD technique becomes closer to the analytical curve as the size q of the partial transmission gain matrix increases from 2 to 4.

Table 1 compares the number of multiplications required for various signal detection techniques for asynchronous FMT-based mesh systems. L_f, M, N and $N_{\text{inv}}(q)$ denote the length of transmit/receive filters, the number of subcarriers, the number of FMT symbols per frame and the number of multiplications required for the inversion of a matrix, respectively. In this example, the following parameters are used: $L_f = 22$, $M = 64$, $N = 10$, $N_{\text{inv}}(2) = 8$ and $N_{\text{inv}}(4) = 112$. The number of nodes (U) is 4 or 8. Table 1 shows that the number of multiplications required for CSD is the smallest because one FFT operation is needed per FMT symbol. The number of multiplications for FENSD is linearly proportional to the number of nodes because it requires U FFT operations per FMT symbol. The BiSD requires a smaller number of multiplications than FENSD in the case of $q = 2$ if the number of nodes is >3. Note that the BiSD always performs better than FENSD. The number of multiplications required for BiSD increases as q increases. Computational complexity required for the selection operation [(FSD/BSD or BiSD), (FSD or BSD)] in Fig. 5 is also shown in Table 1. Fig. 8 shows the number of multiplications required for each signal detection technique when the number of nodes varies. Although the ZF equalisation is used for the proposed SIC technique in this paper, the minimum mean square error equalisation can be also used for better performance with a slightly higher complexity [14].

Finally, the procedure for choosing a signal detection technique in Section 3.3 is described. Since $\Delta_B - \Delta_F \geq \delta$th, BiSD technique is chosen by following the procedure in Fig. 5. Note that the smallest time delay (Δ_F) and largest time delay (Δ_B) in this example are selected as 0 and $(27/72)T$, respectively. Because BiSD technique

Table 1 Comparison of computational complexity among various signal detection techniques

Signal detection technique		Computational complexity, Number of multiplications	Example, $U = 4$	Example, $U = 8$
CSD		$L_f M\frac{9}{8} + \frac{2}{M}\log_2 M + MN$	2224	2224
FENSD		$U\left(L_f M\frac{9}{8} + \frac{2}{M}\log_2 M + MN\right)$	8897	17794
FSD/BSD		$L_f M\frac{9}{8} + \frac{2}{M}\log_2 M + \left(q^2(N-q+1) + N_{\text{inv}}(q)\right)M$	4400 ($q = 2$), 15920 ($q = 4$)	4400 ($q = 2$), 15920 ($q = 4$)
BiSD		$2\left(L_f M\frac{9}{8} + \frac{2}{M}\log_2 M\right) + \left(q^2(N-q+1) + N_{\text{inv}}(q)\right)M$	5984 ($q = 2$), 17504 ($q = 4$)	5984 ($q = 2$), 17504 ($q = 4$)
selection operation	FSD/BSD or BiSD	0 (multiplication), 1 (addition)	0	0
	FSD or BSD	$2((q-1)^2 M)$	128 ($q = 2$), 1152 ($q = 4$)	128 ($q = 2$), 1152 ($q = 4$)

is chosen for signal detection, the BER curve in Fig. 7 with 'BiSD' corresponds to the performance of the proposed signal detection technique. Computational complexity (number of multiplications) required in this example can be found from Table 1, for example, 17,504 for BiSD with $q = 4$ and 0 for selection process (FSD/BSD or BiSD).

5 Conclusion

In this paper, we proposed FSD, BSD and BiSD techniques to reduce the effect of ISI caused by TDoAs among distributed nodes in an asynchronous FMT-based WMN. The proposed signal detection technique uses the partial matrices of the transmission gain matrix to mitigate the effect of ISI from adjacent symbols. It was shown by simulation that the performance of the proposed signal detection technique (BiSD) approaches the analytical curve as the size q of the partial transmission gain matrix increases. The proposed signal detection technique (BiSD with q equal to 2) was shown to always outperform the conventional ones (CSD and FENSD), with lower computational complexity, as long as the number of nodes is >3.

6 Acknowledgment

This research was supported by the MSIP (Ministry of Science, ICT & Future Planning, Korea, under the ITRC (Information Technology Research Center) support program (NIPA-2014-H0301-14-1015) supervised by the NIPA (National IT Industry Promotion Agency), by Basic Science Research Program through the National Research Foundation of Korea (NRF) funded by the Ministry of Education, Science and Technology (2012005603) and by Chung-Ang University Excellent Student Scholarship.

7 References

1 Akyildiz, I.F., Wang, X.: 'Wireless mesh networks: A survey', *Comput. Netw. (Elsevier)*, 2005, **47**, (4), pp. 445–487
2 Oyman, O., Laneman, J.N., Sandhu, S.: 'Multihop relaying for broadband wireless mesh networks: from theory to practice', *IEEE Trans. Commun.*, 2007, **45**, (11), pp. 116–122
3 Kaltenberger, F., Ghaffar, R., Knopp, R., *et al.*: 'Design and implementation of a single-frequency mesh network using open air interface', *EURASIP J. Wirel. Commun. Netw.*, 2010, pp. 1–12, doi:10.1155/2010/719523
4 Park, C.H., Yoo, H.I., Kim, Y.J., Kwon, D.S., Cho, Y.S.: 'An analysis of TDoA effect for OFDMA-based wireless mesh networks'. IEEE Int. Conf. on Communications (ICC), 2011, pp. 1–4
5 Raghunath, R., Chockalingam, A.: 'SIR analysis and interference cancellation in uplink OFDMA with large carrier frequency and timing offsets', *IEEE Trans. Wirel. Commun.*, 2009, **8**, (5), pp. 2202–2208
6 Kim, J.H., Lim, K.J., Kwon, D.S.: 'Distributed frequency synchronization for global synchronization in wireless mesh networks', *J. World Acad. Sci., Eng. Technol.*, 2012, **6**, (10), pp. 1060–1064
7 Sourour, E., Nakagawa, M.: 'Mutual decentralized synchronization for intervehicle communication', *IEEE Trans. Veh. Technol.*, 1999, **48**, (11), pp. 2015–2027
8 Tonello, A.M., Pecile, F.: 'Analysis of the robustness of filtered multitone modulation schemes over satellite channels'. Satellite Communications and Navigation Systems (Signals and Communication Technology), 2008, pp. 599–612
9 Petrella, A.: 'Synchronization algorithms for FBMC systems'. Ph. D Thesis, Universita Degli Studi Di Napoli Federico II, 2009
10 Tonello, A.M., Pecile, F.: 'Synchronization algorithms and receiver structures for multiuser filter bank uplink system', *EURASIP J. Wirel. Commun. Netw.*, 2009, **2009**, (2), pp. 1–17
11 Benvenuto, N., Tomasin, S., Tomba, L.: 'Equalization methods in OFDM and FMT systems for broadband wireless communications', *IEEE Trans. Commun.*, 2002, **50**, (9), pp. 1413–1418
12 Wang, T.R., Proakis, J.G., Zeidler, J.R.: 'Interference analysis of filtered multitone modulation over time-varing frequency-selective fading channels', *IEEE Trans. Commun.*, 2007, **55**, (4), pp. 717–727
13 Tonello, A.M., Pecile, F.: 'Synchronization algorithms for multiuser filtered multitone (FMT) systems'. Proc. IEEE Vehicular Technology Conf., 2005
14 Choi, Y.S., Voltz, P.J., Cassara, F.A.: 'On channel estimation and detection for multicarrier signals in fast and selective rayleigh fading channels', *IEEE Trans. Commun.*, 2001, **49**, (8), pp. 1375–1387